

Fast Magnetic Field-Enhanced Linear Colloidal Agglutination Immunoassay

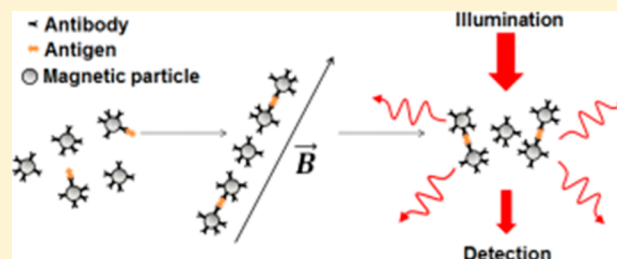
Aurélien Daynès,^{*,†,‡} Nevzat Temurok,[†] Jean-Philippe Gineys,[†] Gilles Cauet,[†] Philippe Nerin,^{†,§} Jean Baudry,[‡] and Jérôme Bibette[‡]

[†]HORIBA ABX SAS, Parc Euromédecine – Rue du Caducée, BP 7290, 34184 Montpellier CEDEX 4, France

[‡]Laboratoire Colloïdes et Matériaux divisés ESPCI, 10 Rue Vauquelin, 75231 Paris, France

S Supporting Information

ABSTRACT: We present the principle of a fast magnetic field enhanced colloidal agglutination assay, which is based on the acceleration of the recognition rate between ligands and receptors induced by magnetic forces.¹ By applying a homogeneous magnetic field of 20 mT for only 7 s, we detect CRP (C-reactive protein) in human serum at a concentration as low as 1 pM for a total cycle time of about 1 min in a prototype analyzer. Such a short measurement time does not impair the performances of the assay when compared to longer experiments. The concentration range dynamic is shown to cover 3 orders of magnitude. An analytical model of agglutination is also successfully



fitting our data obtained with a short magnetic pulse.

Immunoassays consist in quantifying molecules of interest in a biological sample from the detection of complexes formed between a receptor and its ligand. In many assays, receptors are grafted on colloidal particles rather than macroscopic surfaces.² Because colloidal particles present a large surface/volume ratio, this greatly increases the kinetics of ligand–receptor recognition. Early days assays made use of latex particles, which were able to agglutinate in the presence of the molecule of interest.³ Then aggregates induced by receptor–ligand–receptor bonds are commonly quantified by measuring variations of the optical density. This assay, known as latex agglutination immunoassay, or LAI, can be considered as one of the simplest ones, as shown by its still very broad use today. However, it suffers from a lack of both sensitivity and rapidity. Sensitivity can be largely improved by using heterogeneous approaches, such as ELISA, but at the expense of simplicity, cost, and mostly rapidity.^{4–6} Therefore, several approaches aim today at enhancing the sensitivity of homogeneous immunoassays (performed in only one step) to the picomolar range,^{7–11} and at reducing the time and complexity of their protocols. Therefore, as the demand for faster and easy to use techniques is exploding, assays are expected to evolve toward the quantification of analytes to picomolar concentration range in a few minutes only.^{12–16}

Here we use the previously described principle of the acceleration of the recognition rate between ligands and receptors by magnetic forces¹ to set up a rapid and sensitive homogeneous bioassay applicable to any kind of antigen able to bond simultaneously with two antibodies, as required in the LAI technology. Indeed, under an external magnetic field, superparamagnetic particles form linear chains and as the colloids are maintained in contact by magnetic forces, the colliding frequency between particles is no longer mediated by

translational diffusion. This way, the rate of colloidal aggregation is thus greatly increased. Indeed, association kinetics between ligands and receptors grafted on particles maintained within a colloidal chain has been extensively studied and the principles underlying the agglutination kinetics have been clarified.^{17–19} In particular, it has been shown that within a confined chain, the aggregation time constant depends on both colloidal rotational diffusion and grafted ligands dynamics. Based on this principle, we will determine the dose–response curve and its sensitivity limit in the regime of one short imposed magnetic pulse. This will consist in determining the relation between the antigen (or ligand) concentration and the number of sandwich bonds that form within the self-organized chains during the field pulse. In order to model the whole dose–response curve, we consider the formation of linear clusters only, which can have any size above doublets.²⁰ Indeed, commercially promising immunoassays must cover antigens concentration range as large as possible, which naturally impose to consider the formation of linear clusters larger than doublets.

EXPERIMENTAL SECTION

Preparation of Reagents. C-reactive protein (CRP), a 115 kDa homopentameric protein, has been used as a model antigen, whereas polyclonal antibodies have been used as receptors. Colloids consist of superparamagnetic particles of 200 nm diameter (Carboxyl Adembeads, Ademtech). Polyclonal anti-CRP antibodies (L66616G, Meridian Life Sciences) are covalently immobilized onto the beads using water-soluble

Received: January 22, 2015

Accepted: July 3, 2015

Published: July 14, 2015

carbodiimide mediated chemistry. Briefly, particles are washed and then suspended at a concentration of 1% w/v in a 20 mM MES buffer, pH 6.1, and incubated 10 min with EDC (*N*-(3-(dimethylamino)propyl)-*N'*-ethylcarbodiimide) at a final concentration of 2 g/L. Antibodies are then added at a final concentration of 10 μg per mg of particles and incubated for 2 h at room temperature. To determine the amount of antibodies immobilized on particles, we measure the concentration of unreacted antibodies in the supernatant with a colorimetric method (Bio-Rad protein assay). We calculate that about 9 μg of antibodies per mg of particles are grafted. Particles may be prepared with a higher density of antibodies immobilized. Concentrations of antibodies of 20, 30, or 40 $\mu\text{g}/\text{mg}$ are then introduced. We determine that, respectively, 13, 21, or 28 $\mu\text{g}/\text{mg}$ of antibodies are grafted after 2 h of incubation. Antibody-coated 200 nm particles are dispersed at a final concentration of 0.042% w/v in a 50 mM glycine buffer, pH 8.5, with 0.09% w/v of sodium azide as a preservative.

Samples consist of purified CRP (C7907–26A, USBiological) added to CRP-depleted serum (SF100–2, BBI Solutions). CRP concentration in stock solution is determined with an ABX Pentra 400 (Horiba Medical).

Titration of Samples. An automated device has been built to routinely perform samples titration. At start the setup performs two successive dilutions of the serum samples: 27 μL of serum are mixed with 973.7 μL of ABX Eosinofix and 1 mL of ABX Diluent and 3.96 μL of this initial dilution is then mixed with 70.4 μL of particles in the reaction chamber (PMMA cuvette). The reaction chamber is enlightened by a 650 nm RC-LED (Hamamatsu); transmitted light through an optical pathway of 4 mm is detected by a photodiode (S1223, Hamamatsu). A homogeneous magnetic field generated by an electromagnet is then applied to the reaction medium. Duration and intensity of the magnetic pulse are respectively 7 s and 20 mT. The offset voltage on the photodiode, corresponding to the measured background intensity I_b is determined when the RC-LED is off. The initial transmitted intensity I_0 is measured once the reaction medium is mixed in the reaction chamber but before the magnetic field is applied. The transmitted intensity $I(t)$ is measured during the time of acquisition and the variation of optical density, defined as

$$\Delta\text{OD}(t) = -\log \frac{I(t) - I_b}{I_0 - I_b} \quad (1)$$

is used as the read out signal of the experiment. The whole turnaround time, including rinsing and draining steps for the needles and the tanks, is approximately 1 min. The reaction step, including mixing of the reagents, magnetic pulse and read out, is around 15 s. The final dilution factor of the serum sample is around 1400.

RESULTS AND DISCUSSION

Evolution of Signal with Time. In order to determine the behavior of magnetic particles under a pulse of magnetic field, the optical response of suspensions containing various amounts of CRP is monitored during a magnetization cycle. Results are presented on Figure 1a.

When the magnetic field is turned on we systematically observe a sharp decrease of the optical density (OD), occurring in less than 100 ms, as shown in Figure 1b. Actually, few aggregates are always present within the stock suspension of particles, and this signal may be interpreted as the alignment of

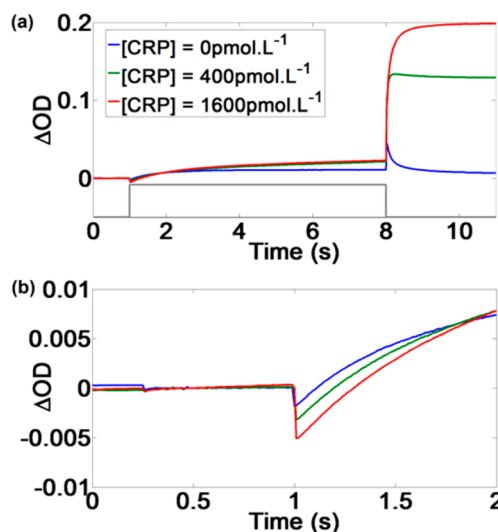


Figure 1. (a) Variation of optical density of particles suspensions submitted to a magnetic field pulse of 7 s, as represented by the gray line. When magnetic field is on, a slow increase of OD is observed, due to particles chaining. When magnetic field is turned off, nonspecific aggregates dissociate, and optical density decreases close to baseline in CRP-free samples. In the presence of CRP, most nonspecific aggregates are dissociated after 3 s of relaxation, whereas CRP-induced specific aggregates are still present; optical density at this time is used to determine CRP concentration. (b) When external field is turned on, pre-existing aggregates align in the direction of the field and a decrease of optical density, dependent on aggregates concentration, is observed.

those aggregates with external field.²¹ We can observe that the OD drop is more pronounced when CRP is added in the medium; this could indicate that CRP aggregates particles even before magnetic field is applied. Nevertheless, this CRP-dependent signal is of the same order of magnitude as nonspecific signal due to particles aggregation in stock solution. We will assume this agglutination is negligible with respect to field-induced aggregation.

While the chaining process occurs, that is, between 1 and 8 s, a slow increase of OD is observed. It appears that increase of OD is higher when CRP is introduced in the medium. The interparticle distance in a chain of nonaggregated particles results from an equilibrium between magnetic attractive and repulsive forces, which determines the optical response of the suspension.²² On the other hand, when a sandwich bond is created between two particles, the interparticle distance is imposed by the length of the bond. Possibly, CRP-induced aggregation modifies the mean interparticle distance in the chains in such a way that optical density is increased.

When the field is turned off, field-induced chains dissociate and Brownian motion tends to disperse the particles, resulting in an increase of OD. We may assume that no local organization induced by magnetic field remains when optical density is maximal. It appears that dispersion occurs with a characteristic time dependent on CRP concentration. Indeed, in blank samples, maximal OD is reached in around 30 ms after the field is turned off. In samples containing CRP, aggregates larger than single particles are present; relaxation then involves both translational and rotational diffusion, and the characteristic time is longer, up to 1 s.

We can observe a slow decrease of optical density for CRP-free samples after the field is turned off, which may be caused

by the dissociation of nonspecific aggregates created during the field pulse. Decay of optical density is not exponential, but can be fitted by a stretched exponential function, $OD(t) = OD_0 \exp[-(t/\tau_0)^\alpha] + OD_\infty$. OD_0 and OD_∞ are, respectively, the initial and final optical densities. τ_0 is the characteristic time of relaxation and α the stretching exponent, from which we can calculate the average relaxation time $\langle\tau\rangle = \tau_0\Gamma(1 + 1/\alpha)$.²³ From our experimental data, we determine $\alpha = 0.40$ and $\tau_0 = 70$ ms, leading to an average time constant of dissociation $\langle\tau\rangle = 230$ ms. Therefore, nonspecific aggregates are nearly completely dissociated few seconds only after magnetic field is switched off. On the other hand, with CRP in the reaction medium, this decrease is no longer observed. Specific antibody-CRP bonds are stable at least several minutes (data not shown). It is thus possible to select a relaxation time long enough to dissociate most nonspecific aggregates, whereas specific bonds are maintained. We decide to use ΔOD after 3 s of relaxation as our read-out signal, for a total measurement time of 11 s.

Dose–Response Curves. Magnetic field-enhanced agglutination assays are performed with samples containing various amounts of CRP ranging from 0 to 6 nM in the reaction medium. Experiments with 0 CRP or 3 pM of CRP are repeated 10 times; other experiments are repeated 5 times. Resulting dose–response curve is presented on Figure 2.

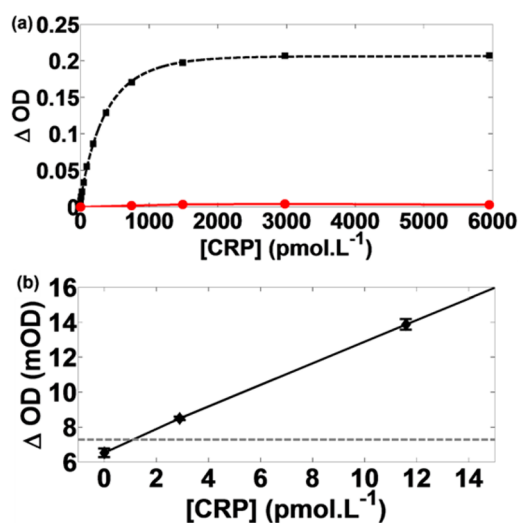


Figure 2. (a) Dose–response curve for our fast magnetic-enhanced agglutination assay; dashed line is the result of the fit. For CRP concentration up to 2 nM, coefficient of variation is less than 10%, and no decrease of signal is observed up to 6 nM. Red circles represent ΔOD measured when no magnetic field is applied; no consequent agglutination is measured. (b) Determination of the limit of detection of the assay. Experimental values of ΔOD are represented with error bars; gray dashed line represents ΔOD for blank assays plus three times standard deviation. This value of ΔOD corresponds to a CRP concentration of 1.1 pM.

We establish that, when particles aggregate within one-dimensional structures only, the number of biological bonds n_b and the number of ligand molecules n_l , each normalized by the number of particles, obey the following law:

$$n_b = 1 - e^{-\rho n_l} \quad (2)$$

where ρ stands for the overall reactivity of the system. Detailed information on this model is provided in the Supporting Information. If we assume that ΔOD is proportional to the

number of links (see Supporting Information), we can then fit our experimental data with the equation:

$$\Delta OD = [MP]\delta_{OD} \left(1 - \exp \left(\exp \left(-\rho \frac{[CRP]}{[MP]} \right) - 1 \right) \right) + OD_{ns} \quad (3)$$

Magnetic particles content is 0.04% w/v within the reaction medium and their molar concentration is $[MP] = 87$ pM. The fitting parameters are δ_{OD} , representing the increase of OD per pM of biological bonds, reactivity ρ , and OD_{ns} which is the background OD contribution due to the remaining nonspecific particles aggregation without any added CRP. Results of the fit give $\delta_{OD} = 3.6$ mOD·pM⁻¹, $\rho = 0.157$ and $OD_{ns} = 8$ mOD. It appears on Figure 2 that the model proposed for magnetic field enhanced agglutination is in good agreement with experimental data for the whole range of CRP concentrations tested. On the other hand, when no magnetic field is applied, agglutination is negligible: a maximum ΔOD of 4 mOD was measured over the range of concentrations used, corresponding to 1 pM only of aggregates formed in 11 s. Without assistance of the magnetic field, detection of such minute quantities of CRP is impossible.

Results of the fit seem quite close to expected values. Indeed, for 200 nm diameter particles of optical index $n = 1.78 - 0.02i$, δ_{OD} is expected to be 4.5 mOD·pM⁻¹ (see Supporting Information). Difference between calculated and experimental results may be due to errors in the value of n or in the actual concentration of particles in the medium. Clusters created in blank assays represent only 2.5% of total particles in the medium. As observed on Figure 1a, 3 s of relaxation allows dissociation of most nonspecific aggregates. Actually, plasmatc proteins other than CRP do not seem to induce consequent aggregation at the dilution rates used in our assay.

We can calculate the limit of detection (LOD), defined as the concentration of CRP giving a signal equal to the blank one plus three times the blank standard deviation. Blank standard deviation is 0.25 mOD, leading to a LOD of 1.1 pM. We determine the upper bound of our assay as the concentration of CRP with an intra-assay coefficient of variation of 10%. We find a concentration of CRP equal to 2 nM, leading to a dynamic antigen concentration range of at least 3 orders of magnitude. A major issue in many agglutination assays may be prozone effect, or hook effect, occurring when antigen is in excess with respect to available antibodies. A competition between capture of antigen and formation of sandwich bonds then occurs, and agglutination is reduced. In our system, no hook effect is observed up to 6 nM of CRP. Duration of the experiment is so short that antibodies are not yet saturated with antigen molecules, even when a large excess of CRP is present. This is confirmed by the fact that the experimental value of ρ is only 16%, indicating that reaction has not reached its equilibrium yet.

If we take into account the dilution factor, the dynamic range of CRP concentration in the serum samples is 0.2–320 mg/L, and no prozone effect is observed up to at least 1 g/L. Physiological levels of CRP are less than 3 mg/L,²⁴ whereas CRP concentration can reach 400 mg/L in bacterial infections.²⁵ Therefore, our system allows the quantification of CRP in serum in most relevant situations.

It may be noticed that the duration of the magnetic pulse and therefore the slope of the dose–response curve are lower than in previous experiments. If we normalize the initial slopes by the optical path length, we obtain for our experiments a slope

of 1.7 mOD per pM of antigen and per cm of optical path, whereas previous experiments, in the regime where doublets only were formed,¹ gave a slope of 6 mOD per pM of antigen and per cm of optical path for 5 min of magnetization. However, the limit of detection lies in the same range, around 1 pM. It seems that our short pulse regime does not notably deteriorate the performances of the assay.

In order to assess reproducibility of our system, 34 measurements for a sample with a theoretical CRP concentration of 40 mg/L have been performed for 11 days. Coefficient of variation for CRP measurements is around 4.5%. Temperature is not regulated in our system; we may thus attribute part of this variation to ambient temperature changes. Therefore, it seems that our method is quite reproducible.

Behavior for Long Magnetization Cycles. Further experiments are performed with a more complex magnetization cycle, consisting of five pulses of 15 s, with a magnetic field intensity of 20 mT, followed by 20 s of relaxation between each magnetic pulse. Once again, ΔOD is plotted versus CRP concentration in the medium. Experiments with 0 CRP or 3 pM CRP are repeated 10 times, other experiments are repeated 3 times. Results are presented on Figure 3.

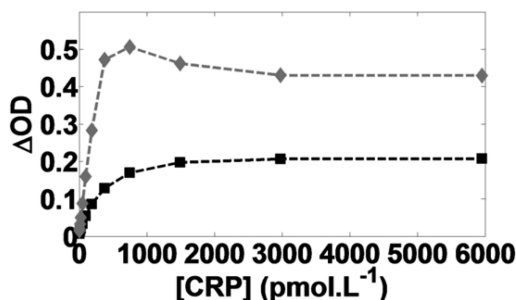


Figure 3. Dose–response curves for different magnetization patterns. Black squares represent short cycle consisting in one pulse of 7 s; gray diamonds represent long cycle consisting in five pulses of 15 s. When a long magnetization cycle is used, ΔOD is higher than previously observed with short pulses. However, for high concentrations, OD is decreased when CRP concentration is increased.

The shape of the dose–response curve is modified for a longer magnetization cycle: ΔOD reaches a much higher value than the plateau value of 210 mOD obtained for short cycle. Furthermore, the linear agglutination model does not fit experimental data anymore. A maximum ΔOD of 500 mOD is observed for $[CRP] = 800$ pM, then ΔOD decreases when the concentration of CRP is increased. The observed phenomenon is quite similar to prozone effect. However, we estimate the mean number of active antibodies in our experiments to be around 28 antibodies per particle (see Supporting Information). Therefore, even if we assume that capture of CRP by the antibodies is completed during the reaction, hook effect should not occur for CRP concentrations lower than at least 1.2 nM. To determine the origin of this phenomenon, assays are then performed with various concentrations of antibodies immobilized on the particles. It is expected that the prozone effect would occur for higher CRP concentrations when more antibodies are present on the particles. However, on Figure 4 we observe that the decrease of OD is more important when more antibodies are immobilized on the particles. Thus, prozone effect is definitely not responsible of the decrease of OD.

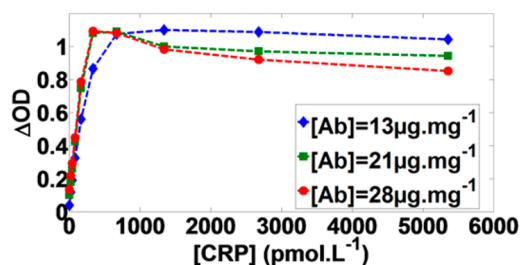


Figure 4. Dose–response curves obtained with various quantities of antibodies immobilized on particles. The optical path is 1 cm. Decrease of ΔOD when high concentrations of CRP are present is more important for higher amounts of antibodies; therefore, it is not due to prozone effect.

Microscopic observations of aggregates are performed for reaction media containing 6 nM of CRP. Pictures can be observed on Figure 5.

When one magnetization pulse of 7 s long is applied, only short aggregates are formed, in concordance with our linear agglutination model. However, for a long magnetization cycle, nonlinear aggregates can be observed, whose size is in the micrometer range. Those aggregates may be formed during

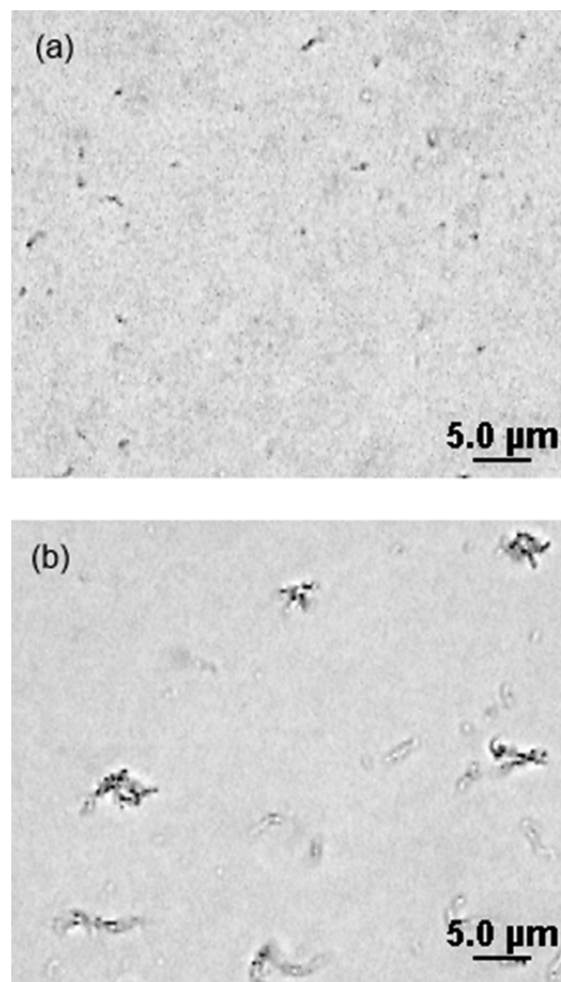


Figure 5. Microscope pictures of agglutinated particles induced by 6 nM of CRP. (a) Agglutination after 1 magnetization pulse: only small aggregates are observed; (b) Agglutination after 5 magnetization pulses: large, nonlinear aggregates are formed.

relaxation steps; when the magnetic field is off, particles move freely in the volume as in a latex agglutination immunoassay and growing aggregates can take any form. If we approximate those aggregates as spheres, Mie theory shows that, when aggregates larger than 1 μm are created, ΔOD is expected to decrease (see Supporting Information). Thus, nonlinear aggregates are likely responsible for the decrease of OD as observed in our assays.

The LOD has been determined for this longer assay. Standard deviation of the blank assays is 1.0 mOD, and the LOD is 1.8 pM. Despite a higher slope of the dose–response curve with respect to the short pulse regime, the performances are not enhanced. It seems that fluctuations of the signal are increased during a longer cycle. Furthermore, due to aforementioned optical effects, no CRP concentration higher than 300 pM can be determined. Above that range, a measured ΔOD may correspond to two different CRP concentrations. Therefore, we observe that a much larger dynamic range is achieved with our short pulse format.

CONCLUSIONS

The use of a magnetic field allows significant increase of the agglutination kinetics in immunoassays, as previously described.¹ Here we show that a limit of detection of around 1 pM of antigen can be achieved for a measurement duration time of 15 s. Moreover the dynamic range is found to reach more than 3 orders of magnitude. By considering linear aggregates only we develop a theoretical model of the agglutination process, which accurately fit our experimental data.

Detection of CRP is thus achieved at physiological levels with a considerable dilution of the sample. Nonspecific aggregation due to biological medium is certainly greatly reduced by such a dilution. However, allowing some relaxation time before measuring the optical density difference clearly helps in dissociating nonspecific aggregates while specific bonds are maintained. This feature may improve the detection limit of proteins when a large dilution of the sample is not possible.

Interestingly, increasing the reaction time itself under field does not improve the performances of the assay: the background noise of the assay is increased, thus no enhancement of the limit of detection is observed. Furthermore, the dynamic range of the assay is much larger when using a single short pulse. Indeed, by increasing the reaction time, a prozone-like effect, apparently induced by the formation of nonlinear aggregates of particles occurs at high concentrations of antigen. Therefore, it appears that our magnetic agglutination assay is ideally suited for a fast readout applied to detection of proteins from picomolar up to nanomolar range. We believe such features are particularly suitable to implement high throughput measurements for in vitro diagnostic technologies.

ASSOCIATED CONTENT

Supporting Information

Additional supporting details. The Supporting Information is available free of charge on the ACS Publications website at DOI: 10.1021/acs.analchem.5b00279.

AUTHOR INFORMATION

Corresponding Author

*E-mail: aurelien.daynes@horiba.com.

Present Address

[§]SAT AxLR, Place Eugène Bataillon, 34095 Montpellier Cedex 5, France. E-mail: philippe.nerin@axlr.com (N.P.).

Notes

The authors declare no competing financial interest.

ACKNOWLEDGMENTS

This work was partially supported by Bpifrance Innovation Stratégie Industrielle (project Dat@Diag).

REFERENCES

- (1) Baudry, J.; Rouzeau, C.; Goubault, C.; Robic, C.; Cohen-Tannoudji, L.; Koenig, A.; Bertrand, E.; Bibette, J. *Proc. Natl. Acad. Sci. U. S. A.* **2006**, *103* (44), 16076–16078.
- (2) Teste, B.; Descroix, S. *Nanomedicine* **2012**, *7* (6), 1917–1923.
- (3) Singer, J. M.; Plotz, C. M. *Am. J. Med.* **1956**, *21* (6), 888–892.
- (4) Grubisha, D. S.; Lipert, R. J.; Park, H. Y.; Driskell, J.; Porter, M. D. *Anal. Chem.* **2003**, *75* (21), 5936–5943.
- (5) Osterfeld, S. J.; Yu, H.; Gaster, R. S.; Caramuta, S.; Xu, L.; Han, S. J.; Hall, D. A.; Wilson, R. J.; Sun, S.; White, R. L.; Davis, R. W.; Pourmand, N.; Wang, S. X. *Proc. Natl. Acad. Sci. U. S. A.* **2008**, *105* (52), 20637–20640.
- (6) Rissin, D. M.; Kan, C. W.; Campbell, T. G.; Howes, S. C.; Fournier, D. R.; Song, L.; Piech, T.; Patel, P. P.; Chang, L.; Rivnak, A. J.; Ferrell, E. P.; Randall, J. D.; Provuncher, G. K.; Walt, D. R.; Duffy, D. C. *Nat. Biotechnol.* **2010**, *28* (6), 595–599.
- (7) Hirsch, L. R.; Jackson, J. B.; Lee, A.; Halas, N. J.; West, J. L. *Anal. Chem.* **2003**, *75* (10), 2377–2381.
- (8) Moser, Y.; Lehnert, T.; Gijs, M. A. M. *Lab Chip* **2009**, *9* (22), 3261–3267.
- (9) Lan, T.; Dong, C.; Huang, X.; Ren, J. *Analyst* **2011**, *136* (20), 4247–4253.
- (10) Lee, J. S.; Joung, H. A.; Kim, M. G.; Park, C. B. *ACS Nano* **2012**, *6* (4), 2978–2983.
- (11) Tian, J.; Zhou, L.; Zhao, Y.; Yang, W.; Peng, Y.; Zhao, S. *Talanta* **2012**, *92*, 72–77.
- (12) Bruls, T. M.; Evers, T. H.; Kahlman, J. A. H.; Van Lankvelt, P. J. W.; Ovsyankuren, M.; Pelssers, E. G. M.; Schleipen, J. J. H. B.; De Theije, F. K.; Verschuren, C. A.; Van der Wijk, T.; van Zon, J. B. A.; Dittmer, W. U.; Immink, A. H. J.; Nieuwenhuis, J. H.; Prins, M. W. J. *Lab Chip* **2009**, *9* (24), 3504–3510.
- (13) Kreisig, T.; Hoffmann, R.; Zuchner, T. *Anal. Chem.* **2011**, *83* (11), 4281–4287.
- (14) Ranzoni, A.; Schleipen, J. J. H. B.; van IJendoorn, L. J.; Prins, M. W. J. *Nano Lett.* **2009**, *9* (22), 2017–2022.
- (15) Chen, C.; Wu, J. *Sensors* **2012**, *12* (9), 11684–11696.
- (16) Oh, Y. K.; Joung, H. A.; Kim, S.; Kim, M. G. *Lab Chip* **2013**, *13* (5), 768–772.
- (17) Chesla, S. E.; Selvaraj, P.; Zhu, C. *Biophys. J.* **1998**, *75* (3), 1553–1572.
- (18) Lee, N. K.; Johner, A.; Thalmann, F.; Cohen-Tannoudji, L.; Bertrand, E.; Baudry, J.; Bibette, J.; Marques, C. M. *Langmuir* **2008**, *24* (4), 1296–1307.
- (19) Cohen-Tannoudji, L.; Bertrand, E.; Baudry, J.; Robic, C.; Goubault, C.; Pellissier, M.; Johner, A.; Thalmann, F.; Lee, N. K.; Marques, C. M.; Bibette, J. *Phys. Rev. Lett.* **2008**, *100* (10), 108301.
- (20) Ranzoni, A.; Sabatte, G.; Van IJendoorn, L. J.; Prins, M. W. J. *ACS Nano* **2012**, *6* (4), 3134–3141.
- (21) Ramiandrisoa, D.; Brient-Litzler, E.; Daynès, A.; Compain, E.; Bibette, J.; Baudry, J. *New Biotechnol.* **2015**, *32*, 467.
- (22) Dreyfus, R.; Lacoste, D.; Bibette, J.; Baudry, J. *Eur. Phys. J. E: Soft Matter Biol. Phys.* **2009**, *28* (2), 113–123.
- (23) Berberan-Santos, M. N.; Bodunov, E. N.; Valeur, B. *Chem. Phys.* **2005**, *315* (1), 171–182.
- (24) Blake, G. J.; Rifai, N.; Buring, J. E.; Ridker, P. M. *Circulation* **2003**, *108* (24), 2993–2999.
- (25) Clyne, B.; Olshaker, J. S. *J. Emerg. Med.* **1999**, *17* (6), 1019–1025.